

SCIENTIFIC REPORTS



OPEN

Regulation of TFPI α expression by miR-27a/b-3p in human endothelial cells under normal conditions and in response to androgens

Ana B. Arroyo¹, Salam Salloum-Asfar¹, Carlos Pérez-Sánchez², Raúl Teruel-Montoya¹, Silvia Navarro³, Nuria García-Barberá¹, Ginés Luengo-Gil¹, Vanessa Roldán¹, John-Bjarne Hansen⁴, Chary López-Pedraza², Vicente Vicente¹, Rocío González-Conejero^{1,*} & Constantino Martínez^{1,*}

The increased risk of cardiovascular events in older men is multifactorial, but the significant reduction of testosterone levels has been involved. As this hormone regulates the expression of TFPI by unknown mechanisms, we aimed to evaluate the role of miRNAs in the regulation of TFPI α expression under normal conditions and in response to androgens. *In silico* studies allowed the selection of 4 miRNAs as potential TFPI α regulators. Only miR-27a/b-3p significantly reduced TFPI α expression in two endothelial cell lines. Luciferase assays demonstrated a direct interaction between miR-27a/b-3p and TFPI 3'UTR. *Ex vivo* analysis of TFPI and miRNA levels in 74 HUVEC samples from healthy subjects, showed a significant and inverse correlation between TFPI and miR-27a-3p. Moreover, anticoagulant activity of TFPI α from cells supernatants decreased ~30% with miR-27a/b-3p and increased ~50% with anti-miR-27a/b-3p. Interestingly, treatment of EA.hy926 with a physiological dose of dihydrotestosterone (30 nM) significantly increased (~40%) TFPI α expression with a parallel decreased (~50%) of miR-27a/b-3p expression. In concordance, increased levels of miR-27a/b-3p normalized the up-regulation induced by testosterone. Our results suggest that testosterone is a hinge in miR-27/TFPI α regulation axis. Future studies are needed to investigate whether testosterone variations are involved in a miR-27/TFPI α dysregulation that could increase the cardiovascular risk.

Tissue factor pathway inhibitor (TFPI), the natural and primary inhibitor of tissue factor (TF), is a prime candidate to control thrombosis through the regulation of TF¹. Few studies have investigated the mechanisms implicated in TFPI regulation which may be of paramount importance to better define its biology and its role in thrombosis. The variability of TFPI plasma levels due to genetic factors account for almost 50%²⁻⁵, but little is known on other factors, in particular hormones.

During the last years, different groups including ours, have evaluated the role of miRNAs in the regulation of haemostasis⁶, as this regulation may have an impact on the thrombotic aetiology⁷. MicroRNAs (miRNAs), are small non-coding RNAs that regulate protein expression that have been involved in the regulation of many complex biological mechanisms⁸ and in many pathological conditions^{9,10}. Thus, three evidences encourage a deep characterization of the testosterone-miRNA-TFPI triad as a new regulatory axis in endothelial function: (i) experimental studies have shown that testosterone up-regulates TFPI expression in endothelial cells^{11,12}; (ii) low levels of testosterone are associated with low plasma levels of TFPI and an increase of cardiovascular risk¹³⁻¹⁵, and (iii) testosterone induces changes in miRNA expression pattern in prostate cancer cells^{16,17} or muscle^{18,19}.

¹Centro Regional de Hemodonación, University of Murcia, IMIB-Arrixaca, Murcia, Spain. ²Maimonides Institute for Research in Biomedicine of Cordoba (IMIBIC). Reina Sofia University Hospital, University of Cordoba, Cordoba, Spain. ³Medical Research Institute, Hospital Universitario y Politécnico La Fe, Valencia, Spain. ⁴K. G. Jebsen - Thrombosis Research and Expertise Center (TREC), Department of Clinical Medicine, UiT - The Arctic University of Norway, Tromsø, Norway; Division of Internal Medicine, University Hospital of North Norway, Tromsø, Norway. *These authors contributed equally to this work. Correspondence and requests for materials should be addressed to R.G.-C. (email: rocio.gonzalez@carm.es) or C.M. (email: constant@um.es)

3' UTR of TFPI/miRNA alignment		TargetScan score	miRanda miRSVR score	miRWalk				
				DIANAmT	miRDB	PITA	RNA22	PICTAR5
Position 2546-2553 of TFPI 3' UTR hsa-miR-27a-3p	5' ...AAUUAAGUGCAUCUAACUGUGAA... 3' CGCCUUGAAUCGGUGACACUU	-0.36	-0.99	+	+	-	-	+
Position 2546-2553 of TFPI 3' UTR hsa-miR-27b-3p	5' ...AAUUAAGUGCAUCUAACUGUGAA... 3' CGUCUUGAAUCGGUGACACUU	-0.36	-0.99	+	+	-	-	+
Position 865-872 of TFPI 3' UTR hsa-miR-19	5' ...CAGUUAUCAUUAGGAUUUGCACA... 3' AGUCAAAACGUACCUGAACGUGU	-0.15	-0.63	+	+	+	-	-
Position 1040-1047 of TFPI 3' UTR hsa-miR-24	5' ...AUCUUUCAUUUAUUGCUGAGCCA... 3' GACAAGGACGACUUGACUCGGU	-0.15	-0.53	+	+	-	-	+

Table 1. *In silico* search of potential miRNAs able to bind to 3' UTR of TFPI.

Therefore, the purpose of this study was to determine whether TFPI α is regulated by miRNAs through a testosterone-dependent mechanism.

Results and Discussion

miR-27a/b-3p directly bind and regulate the expression of TFPI α . We first sought to identify miRNAs as novel and specific regulatory elements in TFPI 3'UTR. Computational results from the different algorithms showed up 4 miRNA candidates: miR-27a/b-3p, miR-19b and miR-24 (Table 1).

We validated *in silico* results by transfecting EA.hy926 endothelial cells (ECs) with all the miRNA candidates. Only miR-27a/b-3p mimics produced a decrease in both TFPI mRNA and extracellular TFPI α levels (Fig. 1A and B), as well as anti-miR-27a/b-3p produced an increase in TFPI mRNA and extracellular TFPI α levels (Fig. 1C and D). These results were confirmed in another EC type (Fig. 1E–H). To reveal whether the effect of miR-27a/b-3p on TFPI α was direct or indirect, we cloned a fragment of TFPI 3'UTR (NM_006287) into a luciferase vector. As a negative control, we deleted the seed region for miR-27a/b-3p. MiR-27a/b-3p significantly reduced the luciferase activity, whereas no effect was observed with the mutated luciferase vector (Fig. 2). Thus, we here described for the first time that TFPI α is directly regulated by two miRNAs, miR-27a/b-3p in ECs and this post-transcriptional regulation of TFPI α might have consequences on the endothelial functions. Emerging evidences have already pointed toward miRNAs as relevant regulators of haemostatic proteins. For example, TF is regulated by miRNAs from the miR-17~92 cluster in monocytes⁷ and by miR-223 in ECs²⁰. On the other hand, protein S (PS), a cofactor for full length TFPI α ²¹, is regulated by miR-494²². Thus, we can speculate that the regulation of TFPI α , TF, and PS may be exerted by a miRNA hub that modulate the TF/TFPI axis, as it has been described for other signaling pathways^{20,23}. Indeed, *in silico* analyses showed that miR-27a/b-3p could also target TF and PS, although these interactions have to be further demonstrated *in vitro*.

miR-27a-3p inversely correlated with TFPI expression in HUVECs. With the aim to test whether the TFPI:miR-27a/b-3p interaction has physiological consequences, we quantified these transcripts in 74 HUVEC samples (from healthy human donors). By using a correlation model, we found that TFPI mRNA and miR-27a-3p levels were inversely and significantly associated (Fig. 3A). However, we found a lack of agreement between the *in vitro* and *ex vivo* results for miR-27b-3p (Fig. 3B) that may be justified because its expression was 18-fold lower than miR-27a-3p in HUVECs (Fig. 3C), which is in accordance with published results²⁴. Indeed, miR-27a and miR-27b were not correlated (Fig. 3D). Therefore it is expected that, in physiological conditions, the lower concentration of miR-27b-3p in HUVECs may explain its lack of association with TFPI levels and potentially a minor role in regulating TFPI α in ECs. As a control, we evaluated the correlations of miR-19b and miR-24 with TFPI. As expected, no significant correlations were observed (Fig. 3E and F), which strengthen the results obtained for miR-27a-3p. Accordingly, the quantification of miR-27a/b-3p might be of interest in pathological conditions where miRNA deficiency or over-expression may have an important impact²⁵.

miR-27a/b-3p levels modulate the anticoagulant effect of TFPI α . We next investigated the functional relevance of TFPI α regulation by miR-27a/b-3p. TFPI α anticoagulant activity was measured in the supernatant of HUVECs transfected with both miRNAs. Transfection with miR-27a/b-3p significantly decreased TFPI α anticoagulant activity, while anti-miR-27a/b-3p significantly increased TFPI α anticoagulant activity (Fig. 4). These latter observations were further confirmed in EA.hy926 cells transfected with miR-27a-3p (Figure S1). This finding suggests that miR-27a/b-3p levels variations may have an impact on TFPI α functionality. Hypoxic conditions have been described previously to up-regulate miR-27a/b-3p expression²⁶ while infective and inflammatory processes down-regulate their expression^{27,28}. Given the extensive cross-talk between the coagulation and inflammatory systems, TFPI included²⁹, additional studies are certainly needed to reveal the role of miR-27a/b-3p in TFPI α regulation and the impact on their activity under pathological conditions.

TFPI α regulation by testosterone is dependent of miRNA expression. It is described that testosterone increases TFPI mRNA and protein levels^{11,12}. Nevertheless, the specific mechanisms of this regulation are largely unknown. In addition, testosterone may also regulate miRNA expression^{16,19}. Thus, we wondered whether miR-27a/b-3p could be implicated in TFPI regulation by testosterone. We treated EA.hy926 cells with a physiological dose of the main testosterone metabolite, dihydrotestosterone (DHT, 30 nM) and we observed a significant increase of both TFPI mRNA (Fig. 5A) and protein after 24 h (Fig. 5B). Indeed, such doses of DHT decreased miR-27a/b-3p (Fig. 5C and D). These results were also shown in HUVECs (Figure S2). Key enzymes implicated

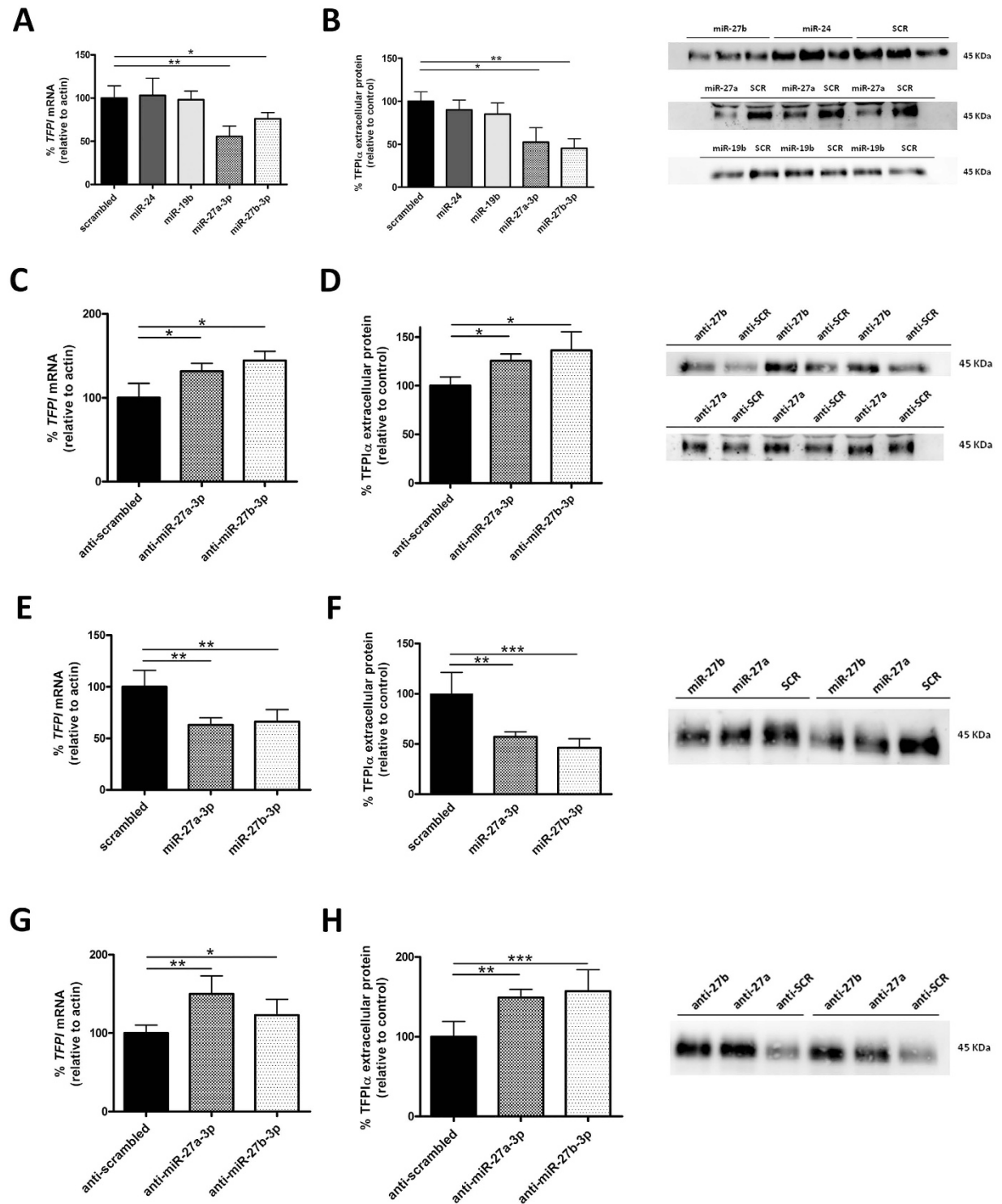


Figure 1. miR-27a/b-3p directly inhibit the expression of TFPI α . Endothelial cells were transfected with different miRNA precursors (100 nM) selected by *in silico* prediction or a scrambled control and mRNA levels were measured after 48 h by qRT-PCR in EA.hy926 (A) and in HUVECs (E). Protein levels in cell culture supernatants were measured by densitometry after western blotting with specific anti-TFPI antibody in EA.hy926 (B) and in HUVECs (F). A representative blot is shown. The TFPI mRNA in EA.hy926 (C) and in HUVECs (G) and the respective protein levels (D,F) of cells transfected with miR-27a/b-3p inhibitors, and determined by the same methods and in the same conditions, is also shown. The $2^{-\Delta Ct}$ method was followed to calculate the relative abundance of mRNA compared with endogenous control expression of β -actin (*ACTB*) ($Ct =$ Threshold Cycle; $\Delta Ct = Ct$ sample gene - Ct endogenous control). For miR-27b and miR-24 the same scrambled control was used. Representative blots are shown. All results are represented as mean \pm SD from at least three experiments performed in triplicate (* $p < 0.05$; ** $p < 0.01$; *** $p < 0.001$).

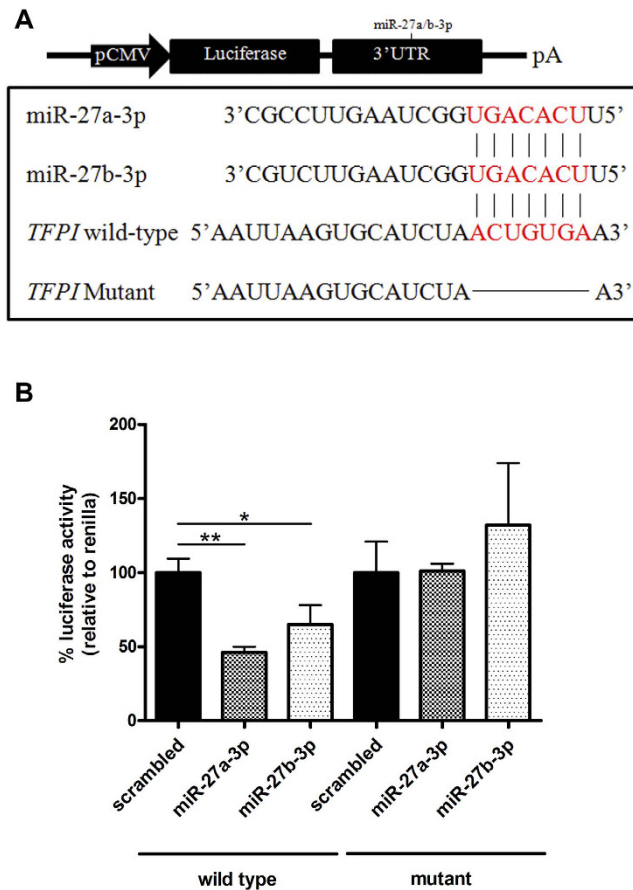


Figure 2. miR-27a/b-3p directly target *TFPI* mRNA. (A) Schematic diagram of the luciferase reporter. Plasmids including *TFPI* WT 3'UTR or *TFPI* mutant 3'UTR in which the seven nucleotides forming the seed region of miR-27a/b-3p were deleted. (B) HTC-DK cells were transfected with either *TFPI* WT 3'UTR or *TFPI* mutant 3'UTR along with 100 nM miR-27a/b-3p precursor. A scrambled precursor was used as control. Luciferase activities were normalized to renilla activities. The $2^{-\Delta Ct}$ method was followed to calculate the relative abundance of mRNA compared with endogenous control expression of β -actin (*ACTB*) ($Ct =$ Threshold Cycle; $\Delta Ct = Ct$ sample gene - Ct endogenous control). All results are represented as mean \pm SD from at least three experiments performed in triplicate (* $p < 0.05$; ** $p < 0.01$).

in the miRNA biogenesis: Drosha, Ago2, Exportin 5, and Dicer were not significantly affected by DHT treatment (Fig. 5E). Therefore, regulation of miR27a/b-3p by testosterone seems to be specific and non-dependent of miRNA biogenesis machinery. Although it has been shown that testosterone increases the rate of pri-miR-27a maturation through the binding of the androgen receptor (AR) to the promoter of the gene in LNCaP prostate cancer cells³⁰, our results showed that DHT provokes a decrease of miR-27a/b-3p in ECs. These results could be partially explained through differences of regulation pathways between both cell types that can certainly have an impact on the miR-27a/b-3p-testosterone regulation³¹. Future studies are needed to investigate whether testosterone variations are involved in a miR-27/TFPI α dysregulation that could increase the cardiovascular risk inherent to aging. However, an important limitation of forthcoming studies will be the accessibility to the adequate samples, e.g. ECs, that can be circumvented by the use of an appropriate animal model.

Finally, combination of androgen treatment with miR-27a/b-3p transfection (Fig. 6A and C) but not with miR-19b or miR-24 (Figure S3) in EA.hy926 cells abolished TFPI up-regulation produced by 30 nM DHT as well as the anticoagulant activity, showing a relationship between testosterone, TFPI, and miR-27a/b-3p. In fact, when ECs transfected with anti-miR-27a/b-3p where treated with 15 nM DHT, we observed a significant increase of TFPI mRNA (Fig. 6B) and of the anticoagulant activity (Fig. 6C) further demonstrating the potential involvement of miR-27a/b-3p in the regulation of TFPI levels in ECs. The effect of miR-27a/b-3p mimics were also shown in HUVECs (Figure S4). Thus, the assessment of therapeutic alternatives with miRNAs may be of interest. This model suggests that in ECs high levels of miR-27a/b-3p might reduce the protective role of testosterone against cardiovascular disease^{14,15}. This situation might be of particular relevance in men with low testosterone levels in relation with age or pathologies such as hypogonadism. Indeed, we hypothesized that miR-27a/b-3p may be upregulated in the plasma of men with low concentration of testosterone and TFPI¹³ in comparison with men with normal levels. Results showed no differences in miR-27a/b-3p expression that may be due to a substantial overlap of TFPI expression between the 2 groups (Fig. 7). Data from higher sample size will help to elucidate the role that miR-27a/b-3p may play in the testosterone mediated downregulation of TFPI *in vivo*, and thus whether

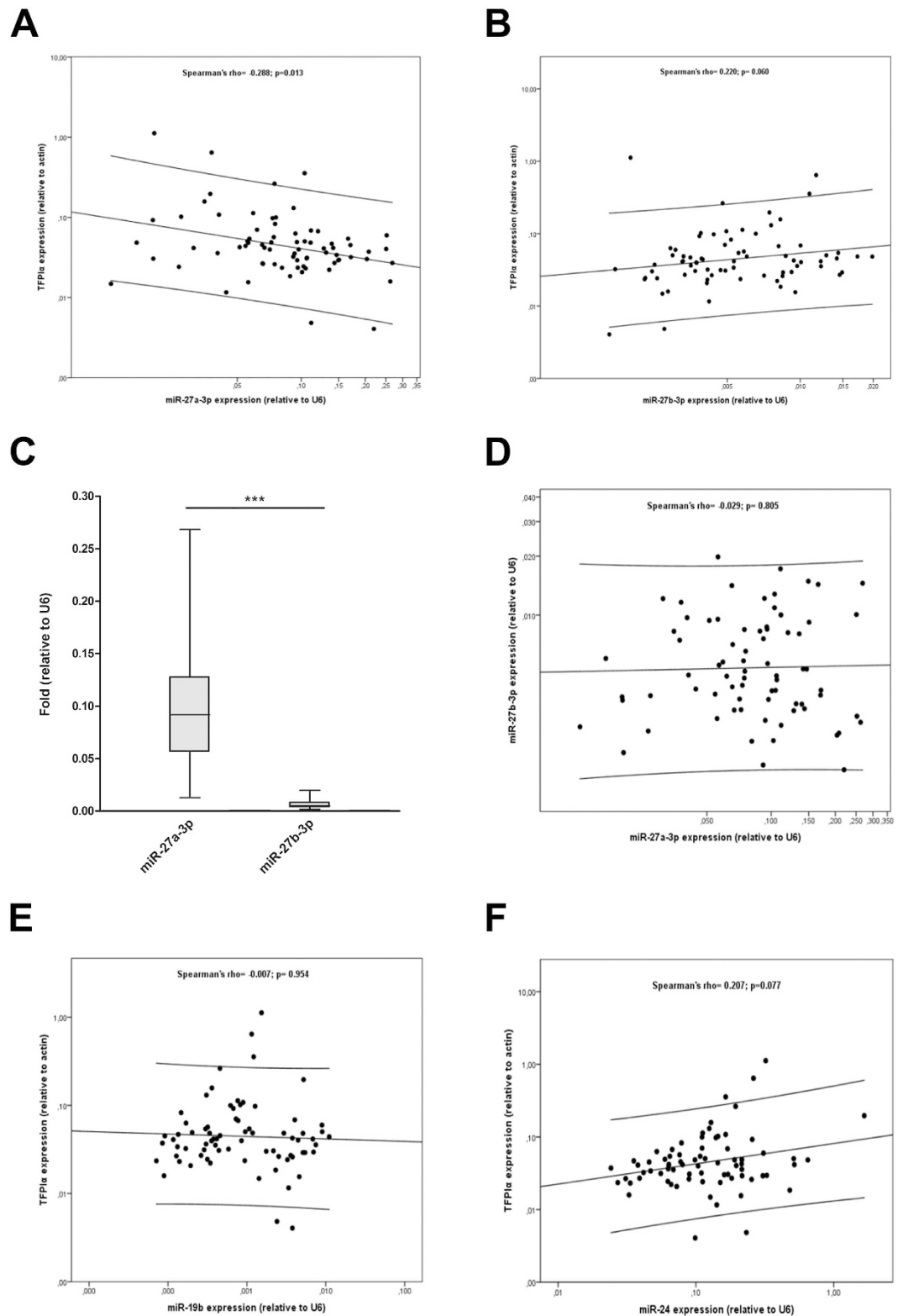


Figure 3. *Ex vivo* expression of *TFPI* mRNA and mature miRNAs. Levels of miR-27a-3p (A), miR-27b-3p (B), miR-19b (E) and miR-24 (F) were measured by qRT-PCR and correlated with *TFPI* mRNA expression in 74 HUVEC samples obtained from umbilical cords. (C) Mean levels of miR-27a/b-3p in HUVECs. (D) correlation between miR-27a-3p and miR-27b-3p. The $2^{-\Delta Ct}$ method was followed to calculate the relative abundance of miRNA compared with endogenous control expression of U6 (Ct = Threshold Cycle; ΔCt = Ct sample gene - Ct endogenous control) (**p < 0.01).

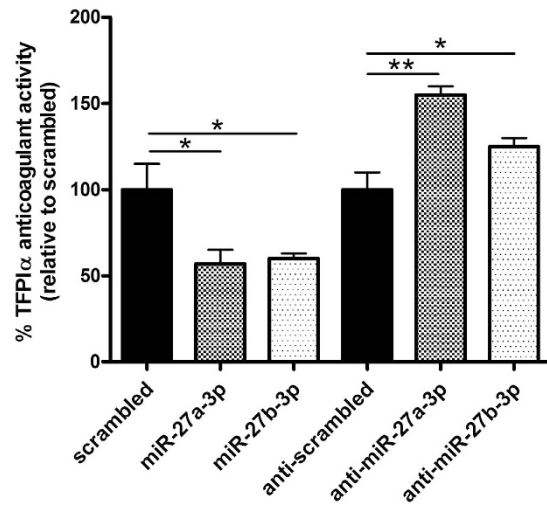


Figure 4. miR-27a/b-3p regulate the anticoagulant activity of TFPI α in HUVECs. TFPI α anticoagulant activity was measured in the supernatant from HUVECs transfected with precursors or inhibitors of miR-27a/b-3p. All results are represented as mean \pm SD from at least three experiments performed in triplicate (* p < 0.05; ** p < 0.01).

it could be a contributing factor to the risk of thrombosis associated with low testosterone levels^{14,15}. In an attempt to further demonstrate the regulation of TFPI by miR-27a/b-3p through testosterone, we compared the levels of miR-27a/b-3p and TFPI mRNA in HUVECs in both genders and found no differences (Figure S5). This can be due because at delivery, even if testosterone levels are higher in boys than in girls these levels are 10 times lower than those found in adult individuals³². Thus, the regulatory role of testosterone in newborns may be probably negligible.

In conclusion, our results showed that miRNAs represent a novel mechanism by which TFPI α , a relevant haemostatic molecule, is modulated in ECs. Further *in vivo* studies must be performed to reveal the real transcendence of our results. We suggest that testosterone may be a hinge in miR-27a/b-3p-TFPI α regulation axis (Fig. 8). Given the high variability of miRNA expression levels among healthy population in different tissues, the pathophysiological consequences of this regulation have yet to be established i.e., risk of cardiovascular disease^{33,34}. In addition, the relevance of our experimental data should be further determined in the context of a potential use of miRNA inhibitors as anti-thrombotic drug.

Methods

***In silico* analysis of TFPI 3'UTR.** To identify miRNA-binding sites located in human TFPI 3'UTR (NM_006287) an *in silico* search using miRNA binding sites prediction programs was performed: miRSVR (<http://www.microrna.org>), TargetScan (<http://www.targetscan.org>), and miWalk (<http://www.umm.uni-heidelberg.de/apps/zmf/mirwalk/>). MiWalk covers five different algorithms (DIANA, miRDB, PITA, RNA22, and PICTAR).

Cell line and tissue samples. Endothelial cell line EA.hy926 was obtained from the American Type Culture Collection (Manassas, VA). ECs were maintained in phenol-red free DMEM supplemented with 2 mM glutamine, and 10% fetal bovine serum (Life Technologies, Madrid, Spain). Human colon cancer cell line HCT-116 deficient for Dicer (HCT-DK) was a kind gift from Dr. Renato Baserga (Thomas Jefferson University, PA). HCT-DK were cultured in McCoy's 5A (Sigma-Aldrich, Madrid, Spain) supplemented with 2 mM glutamine and 10% fetal bovine serum. Umbilical cord samples were obtained from healthy donors that gave informed consent (La Fe Hospital, Valencia, Spain) (n = 74). Studies with human HUVECs were approved by Local Ethics Committee from Hospital Universitario Morales Meseguer in Murcia and performed according to the declaration of Helsinki. Primary cultures of HUVECs were obtained by standard procedures. Briefly, HUVECs were obtained by collagenase digestion from umbilical cords from healthy donors, and were cultured at 37 °C in humidified air containing 5% CO₂. The selection of ECs was performed by filtration. HUVECs were grown to confluence in T-75 flasks precoated with endothelial cell attachment factor (Sigma-Aldrich, Madrid, Spain), in medium M199 1X (+) Earle's, 2mM L-glutamine, 25 mM HEPES, L-aminoacids (Life Technologies, Madrid, Spain), supplemented with 20% fetal bovine serum (Life Technologies, Madrid, Spain), 1% endothelial cell growth factor (ECGF) (Sigma-Aldrich, Madrid, Spain), 1 mM sodium pyruvate, 50 U/mL penicillin, and 50 μ g/mL streptomycin sulphate (Life Technologies, Madrid, Spain). Confluent EC monolayers were harvested from the culture flasks with 0.25% trypsin/EDTA solution/0.02% PBS (Biochrom, Cambridge, UK). Cells to be used for total RNA isolation were stored at -80 °C after adding 5 volumes of RNAlater (Life Technologies, Madrid, Spain). Although we had no direct confirmation that the isolated HUVECs were a pure endothelial culture, each culture was examined using a LEITZ DM-IRB inverted fluorescence research microscope (LEICA, Wetzlar, Germany) to ensure that the morphology was consistent with ECs. In all cases cells were cultured under conditions favoring EC growth

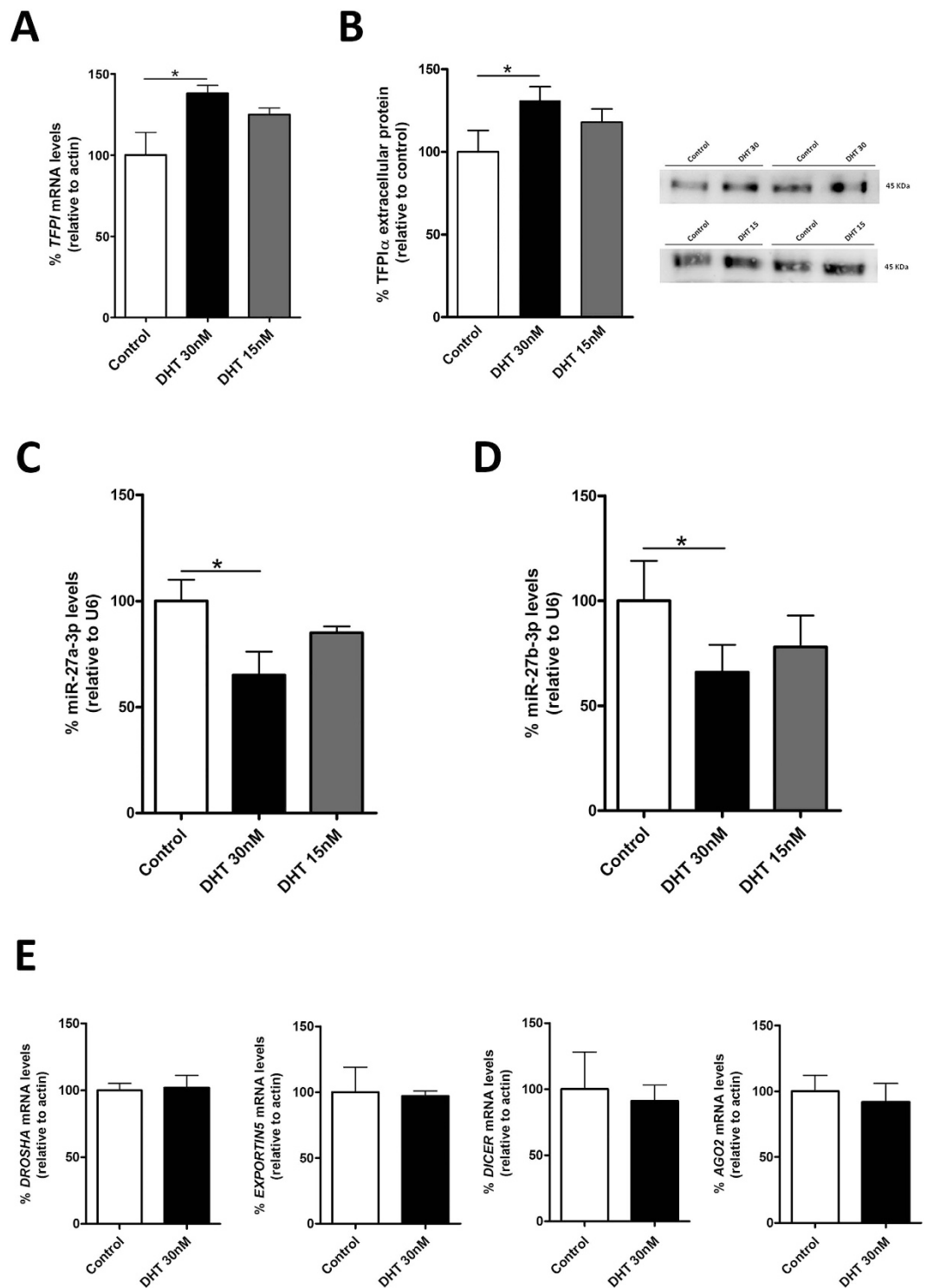


Figure 5. DHT regulates miR-27a/b-3p and TFPI expression. EA.hy926 cells were activated with physiological (30 nM) or low (15 nM) doses of DHT and *TFPI* mRNA (A), secreted TFPI α expression (B) and miR-27a/b-3p levels (C,D) were measured. (E) Levels of mRNA transcripts from enzymes implicated in the miRNA biogenesis: Drosha, Argonaute 2 (AGO2), Exportin 5 and Dicer were measured by qRT-PCR. The $2^{-\Delta\Delta Ct}$ method was followed to calculate the relative abundance of miRNA or mRNA compared with endogenous control expression of U6 or *ACTB* (Ct = Threshold Cycle; $\Delta\Delta Ct$ = Ct sample gene - Ct endogenous control). All results are represented as mean \pm SD from at least three experiments performed in triplicate (* $p < 0.05$).

(medium supplemented with ECGF) and showed the same growth pattern: endothelial-like morphology like as cobblestone-shape area, spindle-shaped cell with cytoplasm distributed homogeneously, without presence of hyperplasia or hill-and-valley morphology, typical for vascular smooth muscle cells culture.

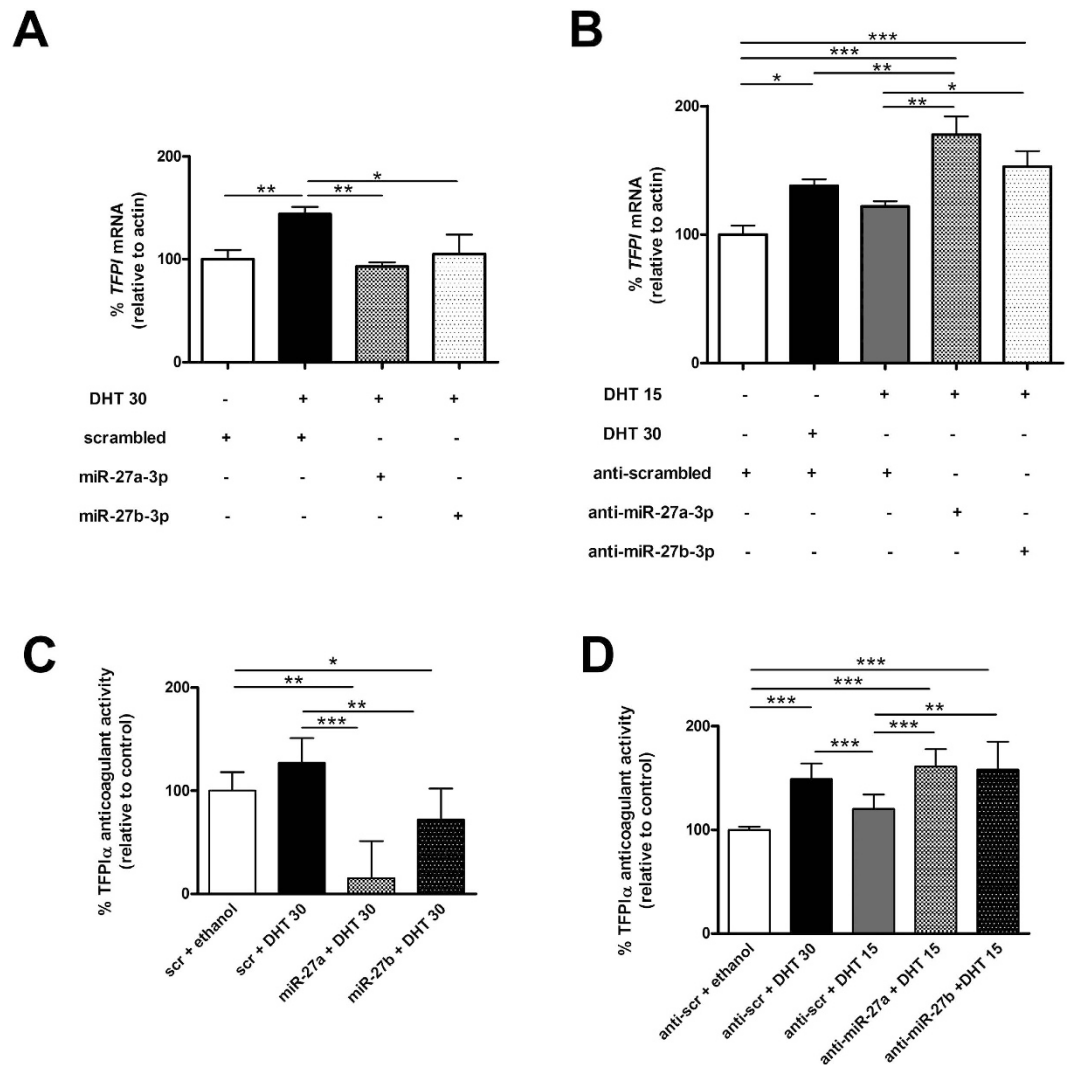


Figure 6. miR-27a/b-3p regulate DHT-dependent TFPI expression. EA.hy926 cells transfected with (A) miR-27a/b-3p precursors or (B) miR-27a/b-3p inhibitors were activated with 15 nM or 30 nM DHT. After 48 h levels of TFPI mRNA were measured by qRT-PCR as well as TFPI anticoagulant activity (C). The $2^{-\Delta Ct}$ method was followed to calculate the relative abundance TFPI mRNA compared with endogenous control expression of *ACTB* (Ct = Threshold Cycle; $\Delta Ct = Ct \text{ sample gene} - Ct \text{ endogenous control}$). All results are represented as mean \pm SD from at least three experiments performed in triplicate (* $p < 0.05$; ** $p < 0.01$; *** $p < 0.001$).

Cells were used within 2–3 passages for all experiments. All the cells were grown at 37°C under 5% CO₂ atmosphere.

Endothelial cells transfections. EA.hy926 and HUVECs were seeded at 50,000/well and transfected with 100 nmol/L miRNA mimics (miR-27a/b-3p, miR-24, miR-19b or scrambled control -SCR-) from Life Technologies (Madrid, Spain) and anti-miRNA inhibitors (anti-miR-27a/b-3p or anti-SCR control) from Exiqon (Vedbaek, Denmark) using siPORT™ NeoFX™ (Life Technologies, Madrid, Spain) according to manufacturer's instructions. After 48 h, cells and supernatants were collected for subsequent mRNA and protein analyses. Expression levels of miRNAs after transfection are shown in Supplemental Figure S6.

Total RNA isolation and qRT-PCR. Total RNA, including miRNAs, was isolated from EA.hy926 and HUVEC with RNazol Reagent (Molecular Research Center Inc, Cincinnati, OH) according to manufacturer's instructions. Isolation of miRNA from plasma was performed with NucleoSpin® miRNA plasma kit (Machery-Nagel, Düren, Germany). Reverse transcription (RT) reaction of total RNA (400 ng) was performed using SuperScript™ III First-Strand Synthesis System (Invitrogen, Madrid, Spain). MiRNA cDNA was synthesized from total RNA purified from cells (200 ng) and from plasma (8 μ L of each sample) using individual miRNA-specific RT primers and the TaqMan® MicroRNA Reverse Transcription Kit (Life Technologies, Madrid, Spain). Each cDNA was amplified using the TaqMan® MicroRNA assays together with TaqMan® Universal PCR

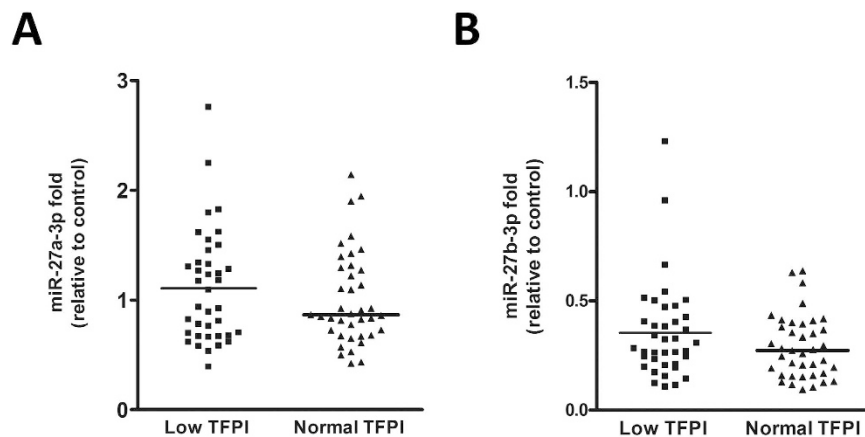


Figure 7. Levels of miR-27a/b-3p in human plasma. (A) miR-27a and (B) miR-27b measured in plasma samples of 70 year-old patients with low TFPI ($n = 37$; 10.9 ± 2.3 ng/L) expression and normal TFPI ($n = 41$; 12.3 ± 3 ng/L) expression¹³. The $2^{-\Delta Ct}$ method was followed to calculate the relative abundance of miR-27a/b compared with control (geometric mean of miR-103-3p and miR-191) ($Ct =$ Threshold Cycle; $\Delta Ct = Ct$ sample gene - Ct endogenous control). Lines indicate population median.

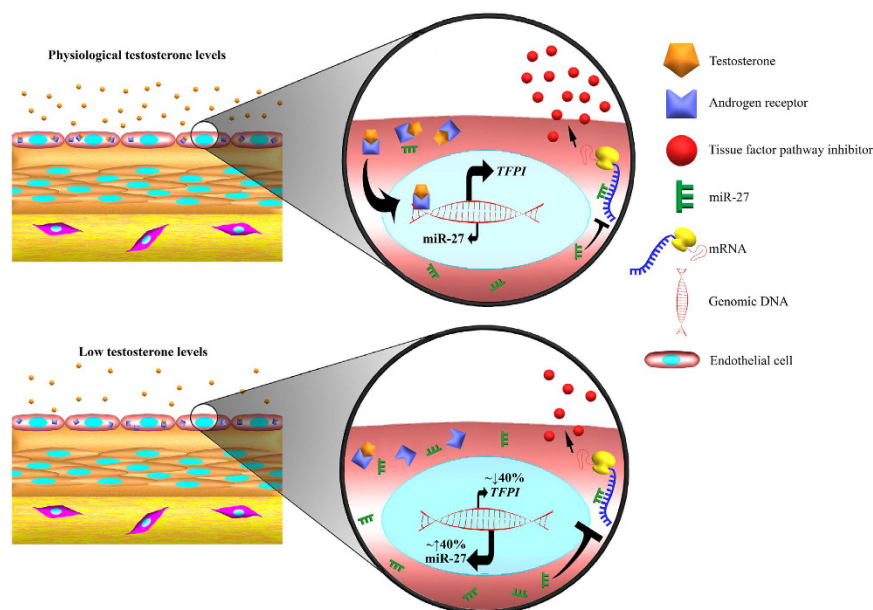


Figure 8. Schematic diagram of the TFPI regulatory mechanism by miRNAs. In the presence of normal levels of testosterone, TFPI expression is regulated in part by the presence of miR-27a/b in the cytosolic compartment. In physiological or pathological conditions where testosterone levels decrease, TFPI expression is downregulated due to a lower transcription of TFPI mRNA but also to a higher repression by miR-27a/b.

Master Mix, No AmpErase[®] UNG (Life Technologies, Madrid, Spain). The $2^{-\Delta Ct}$ method was followed to calculate the relative abundance of miRNA and mRNA compared with endogenous control expression, U6 for cells miRNA and *ACTB* for mRNA. Plasma miRNA was normalized with geometric mean of miR-103-3p and miR-191 ($Ct =$ Threshold Cycle; $\Delta Ct = Ct$ sample gene - Ct endogenous control).

Western blotting and antibodies. Cell supernatants were collected from 24-well plates and BCA assays (ThermoFisher Scientific, Madrid, Spain) were performed to calculate protein concentration of samples. Protein concentration variability between samples was low ($4.8\text{--}5.5$ $\mu\text{g}/\mu\text{L}$ for EAhy.926 and $1.3\text{--}1.6$ $\mu\text{g}/\mu\text{L}$ for HUVEC). Normalization in the western blot was based on the amount of protein loaded. For this purpose, 100 μg (EAhy.926) and 30 μg (HUVEC) of total protein was separated by SDS-PAGE in reducing conditions by electrophoresis in 8% polyacrylamide gels. Gels were transferred onto PVDF membranes (Amersham Hybond P 0.45, GE Healthcare, Barcelona Spain) and blocked 1 hour in 5% w/v non-fat drymilk. Antibody against human TPFI (#ADG72, Sekisui Diagnostics, Rüsselsheim, Germany) was used 1:5,000 dilution and incubated overnight at 4°C . The secondary antibody labeled with peroxidase (GE Healthcare, Barcelona, Spain) was used 1:10,000. ECL

Prime Detection Kit and ImageQuant LAS 4000 Imager (GE Healthcare, Barcelona, Spain) were used for sample detection. Densitometric analyses were performed with ImageJ software (<http://rsb.info.nih.gov/ij/>). Linearity between the amount of sample and densitometry was assessed ($r^2 = 0.95$). Data were expressed as changes relative to cells transfected with SCR, taken as 100%.

Plasmid construction and deletion mutagenesis. PCR product (198 bp) containing a fragment of *TFPI* 3'UTR (NM_006287) with miR-27a/b-3p binding site was cloned into pCR 2.1 vector (Life Technologies, Madrid, Spain) using the primers: (5'GAGCTCCGTTATTTTACCGTGTTTTG and 5'ACGCGTCGTTGAGTGGTTTTTCAG). *SacI* and *MluI* were used to digest positive clones (New England Biolabs, Ipswich, MA). The insert was subcloned into luciferase reporter plasmid pMIR-REPORT (Life Technologies, Madrid, Spain) previously digested with these enzymes. A deletion mutant of pMIR-REPORT-TFPI without miR-27a/b-3p seed region-binding site was generated using the primers S: 5'GAGCTCCGTTATTTTACCGTGTTTTG and AS: 5'ACGCGTCGTTGAGTGGTTTTTCAG with the QuikChange site-directed mutagenesis kit (Agilent Technologies, Santa Clara, CA). Insertion of TFPI 3' UTR fragment and seed sequence deletion was confirmed by sequencing. PCR amplification was performed on plasmid DNA (Platinum Taq High Fidelity, Life Technologies, Madrid, Spain) and cleaned-up using ExoSAP-IT (Affymetrix, Santa Clara, CA). Sequences were performed using the BigDye Terminator Reaction Chemistry v3.1 on Applied Biosystems 3130 XL DNA analyzers (Life Technologies, Madrid, Spain). Alignments and sequence analysis were performed using Seqman Pro program (Lasergene version 7.1, DNASTAR, Madison, WI).

Luciferase assay. HCT-DK cells were co-transfected with miR-27a/b-3p (both pMIR-REPORT plasmids –500 ng/well-wild type or mutated for the miR-27a/b-3p seed site) or SCR control, and 50 ng/well of renilla luciferase control plasmid (pRL-TK; Promega, Madison, WI) using Lipofectamine LTX (Life Technologies) according to the manufacturer's instructions. After transfection (48 h), firefly and renilla luciferase activities were measured using the Dual-Glo Luciferase Reporter Assay (Promega, Madison, WI) in a Synergy 2 luminometer (Biotek, Winooski, VT).

TFPI α functional assay. The inhibitory activity of TFPI α was measured by functional chromogenic assay on supernatants from transfected cells (EAhy.926 and HUVECs), where TF-FVIIa dependent FXa generation was quantified using Actichrome[®] TFPI activity assay kit (Sekisui Diagnostics, Rüsselsheim, Germany) following manufacturer's protocol. Briefly, 20 μ L of culture supernatant (adjusted by BCA method to optimal concentration depending on cell line) were added into the wells of a micro-test plate. Then, 20 μ L of FVIIa/TF complex were added and incubated at 37 °C for 30 min. After that, 20 μ L of human FX were added into each well and incubated for 15 min. After adding 20 μ L of EDTA, the reaction was initiated by adding 20 μ L of spectrozyme FXa substrate. Absorbance was read at 405 nm in a spectrophotometer for 10 min and V_{max} was calculated.

Endothelial cells treatment. EA.hy926 and HUVEC cells pre-incubated for 48 h with 10% steroid-free FBS (charcoal/dextran-stripped serum from GE Hyclone, Logan, UT) were treated for 24 h with 15 nM or 30 nM (physiologic concentration) dihydrotestosterone (DHT) (Sigma-Aldrich, Madrid, Spain) or 0.1% ethanol (vehicle control).

Statistical analysis. Statistical analysis was performed with SPSS 21.0 (SPSS, Inc., Chicago, IL, USA) and GraphPad Prism 3.0 (GraphPad Software, Inc., La Jolla, CA, USA). For two groups comparisons, non-parametric test (U Mann–Whitney) was used. For multiple comparisons, one-way ANOVA on ranks with a post-hoc test (Bonferroni correction) were used. Association between continuous variables was analyzed by the Spearman's rank correlation coefficient. Normal distribution of each variable was analyzed using one sample Kolmogorov–Smirnov test with Lilliefors significance correction. Results were expressed as mean \pm SD. All tests were two-sided, and statistical significance was defined as a p -value < 0.05 (or smaller for corrected p -values in multiple comparisons).

References

- Winckers, K., ten, C. H. & Hackeng, T. M. The role of tissue factor pathway inhibitor in atherosclerosis and arterial thrombosis. *Blood Rev.* **27**, 119–132 (2013).
- Almasy, L. *et al.* A locus on chromosome 2 influences levels of tissue factor pathway inhibitor: results from the GAIT study. *Arterioscler. Thromb. Vasc. Biol.* **25**, 1489–1492 (2005).
- Warren, D. M. *et al.* Heritability of hemostasis phenotypes and their correlation with type 2 diabetes status in Mexican Americans. *Hum. Biol.* **77**, 1–15 (2005).
- Bladbjerg, E. M. *et al.* Genetic influence on thrombotic risk markers in the elderly—a Danish twin study. *J. Thromb. Haemost.* **4**, 599–607 (2006).
- Dennis, J., Kassam, I., Morange, P. E., Tregouet, D. A. & Gagnon, F. Genetic determinants of tissue factor pathway inhibitor plasma levels. *Thromb. Haemost.* **114**, 245–257 (2015).
- Teruel-Montoya, R., Rosendaal, F. R. & Martínez, C. MicroRNAs in hemostasis. *J. Thromb. Haemost.* **13**, 170–181 (2015).
- Teruel, R. *et al.* Identification of miRNAs as potential modulators of tissue factor expression in patients with systemic lupus erythematosus and antiphospholipid syndrome. *J. Thromb. Haemost.* **9**, 1985–1992 (2011).
- Bartel, D. P. MicroRNAs: target recognition and regulatory functions. *Cell* **136**, 215–233 (2009).
- Van, R. K., Pollet, J. & Calin, G. A. miRNAs and long noncoding RNAs as biomarkers in human diseases. *Expert. Rev. Mol. Diagn.* **13**, 183–204 (2013).
- Quiat, D. & Olson, E. N. MicroRNAs in cardiovascular disease: from pathogenesis to prevention and treatment. *J. Clin. Invest.* **123**, 11–18 (2013).
- Jin, H. *et al.* Physiological testosterone stimulates tissue plasminogen activator and tissue factor pathway inhibitor and inhibits plasminogen activator inhibitor type 1 release in endothelial cells. *Biochem. Cell Biol.* **85**, 246–251 (2007).

12. Lupu, C., Zhu, H., Popescu, N. I., Wren, J. D. & Lupu, F. Novel protein ADTRP regulates TFPI expression and function in human endothelial cells in normal conditions and in response to androgen. *Blood* **118**, 4463–4471 (2011).
13. Agledahl, I., Brodin, E., Svartberg, J. & Hansen, J. B. Plasma free tissue factor pathway inhibitor (TFPI) levels and TF-induced thrombin generation *ex vivo* in men with low testosterone levels. *Thromb. Haemost.* **101**, 471–477 (2009).
14. Khaw, K. T. *et al.* Endogenous testosterone and mortality due to all causes, cardiovascular disease, and cancer in men: European prospective investigation into cancer in Norfolk (EPIC-Norfolk) Prospective Population Study. *Circulation* **116**, 2694–2701 (2007).
15. Haring, R. *et al.* Low serum testosterone levels are associated with increased risk of mortality in a population-based cohort of men aged 20–79. *Eur. Heart J.* **31**, 1494–1501 (2010).
16. Waltering, K. K. *et al.* Androgen regulation of micro-RNAs in prostate cancer. *Prostate* **71**, 604–614 (2011).
17. Wang, W. L., Chatterjee, N., Chittur, S. V., Welsh, J. & Tenniswood, M. P. Effects of 1 α , 25 dihydroxyvitamin D3 and testosterone on miRNA and mRNA expression in LNCaP cells. *Mol. Cancer* **10**, 58 (2011).
18. Narayanan, R. *et al.* MicroRNAs are mediators of androgen action in prostate and muscle. *PLoS One* **5**, e13637 (2010).
19. Nielsen, S. *et al.* Muscle specific miRNAs are induced by testosterone and independently upregulated by age. *Front. Physiol.* **4**, 394 (2013).
20. Li, Y. *et al.* Comprehensive analysis of the functional microRNA-mRNA regulatory network identifies miRNA signatures associated with glioma malignant progression. *Nucleic Acids Res.* **41**, e203 (2013).
21. Hackeng, T. M., Sere, K. M., Tans, G. & Rosing, J. Protein S stimulates inhibition of the tissue factor pathway by tissue factor pathway inhibitor. *Proc. Natl. Acad. Sci. USA* **103**, 3106–3111 (2006).
22. Tay, J. W., Romeo, G., Hughes, Q. W. & Baker, R. I. Micro-Ribonucleic Acid 494 regulation of protein S expression. *J. Thromb. Haemost.* **11**, 1547–1555 (2013).
23. Vickers, K. C. *et al.* MicroRNA-27b is a regulatory hub in lipid metabolism and is altered in dyslipidemia. *Hepatology* **57**, 533–542 (2013).
24. Kuehbachner, A., Urbich, C., Zeiher, A. M. & Dimmeler, S. Role of Dicer and Drosha for endothelial microRNA expression and angiogenesis. *Circ. Res.* **101**, 59–68 (2007).
25. Mendell, J. T. & Olson, E. N. MicroRNAs in stress signaling and human disease. *Cell* **148**, 1172–1187 (2012).
26. Lin, Q., Gao, Z., Alarcon, R. M., Ye, J. & Yun, Z. A role of miR-27 in the regulation of adipogenesis. *FEBS J.* **276**, 2348–2358 (2009).
27. Buck, A. H. *et al.* Post-transcriptional regulation of miR-27 in murine cytomegalovirus infection. *RNA*. **16**, 307–315 (2010).
28. Xie, N. *et al.* miR-27a regulates inflammatory response of macrophages by targeting IL-10. *J. Immunol.* **193**, 327–334 (2014).
29. Maroney, S. A. & Mast, A. E. Tissue factor pathway inhibitor and bacterial infection. *J. Thromb. Haemost.* **9**, 119–121 (2011).
30. Fletcher, C. E. *et al.* Androgen-regulated processing of the oncomir miR-27a, which targets Prohibitin in prostate cancer. *Hum. Mol. Genet.* **21**, 3112–3127 (2012).
31. Pomerantz, M. M. *et al.* The androgen receptor cistrome is extensively reprogrammed in human prostate tumorigenesis. *Nat. Genet.* **47**, 1346–1351 (2015).
32. Tomlinson, C. *et al.* Testosterone measurements in early infancy. *Arch. Dis. Child. Fetal Neonatal Ed.* **89**, F558–F559 (2004).
33. Teruel-Montoya, R. *et al.* MicroRNA expression differences in human hematopoietic cell lineages enable regulated transgene expression. *PLoS One* **9**, e102259 (2014).
34. Salloum-Asfar, S. *et al.* Regulation of Coagulation Factor XI Expression by MicroRNAs in the Human Liver. *PLoS One* **9**, e111713 (2014).

Acknowledgements

The authors thank Dr Renato Baserga, Department of Cancer Biology, Thomas Jefferson University, for kindly providing us HCT116-Dicer KO cells. The authors thank Javier Corral for reviewing the paper and María del Mar Sánchez Vera for technical expertise. This work was supported by research grants from the Instituto de Salud Carlos III and Fondo Europeo de Desarrollo Regional (FEDER) [PI14/00253, Red RIC (RD12/0042/0050)], and 19873/GERM/15 (Fundación Séneca). A.B.A. has a research Fellowship from University of Murcia. C.M. is an investigator from the Fundación para la Formación e Investigación Sanitarias de la Región de Murcia (FFIS).

Author Contributions

A.B.A. performed the experiments, analyzed and interpreted data. S.S.-A. performed correlation studies in HUVEC and luciferase assays. C.P.-S. performed the pilot study of miR-27a-3p regulation of *TFPI* in EA.hy926 cells. R.T.-M. contributed to the writing of the manuscript. S.N. isolated HUVECs from umbilical cords. N.G.-B. performed the experiments. G.L.-G. performed Supplemental Figures S3 and S4. V.R. performed statistical analyses. J.-B.H. provided plasma samples and critically read the manuscript. C.L.-P. and V.V. critically read the manuscript. R.G.-C. and C.M. designed the research, analyzed data and co-wrote the manuscript.

Additional Information

Supplementary information accompanies this paper at <http://www.nature.com/srep>

Competing financial interests: The authors declare no competing financial interests.

How to cite this article: Arroyo, A.B. *et al.* Regulation of *TFPI* expression by miR-27a/b-3p in human endothelial cells under normal conditions and in response to androgens. *Sci. Rep.* **7**, 43500; doi: 10.1038/srep43500 (2017).

Publisher's note: Springer Nature remains neutral with regard to jurisdictional claims in published maps and institutional affiliations.



This work is licensed under a Creative Commons Attribution 4.0 International License. The images or other third party material in this article are included in the article's Creative Commons license, unless indicated otherwise in the credit line; if the material is not included under the Creative Commons license, users will need to obtain permission from the license holder to reproduce the material. To view a copy of this license, visit <http://creativecommons.org/licenses/by/4.0/>

© The Author(s) 2017